Thermodynamics of Activation Gating in Olfactory-Type Cyclic Nucleotide-Gated (CNGA2) Channels

Vasilica Nache,* Jana Kusch,* Christoph Biskup,* Eckhard Schulz,† Thomas Zimmer,* Volker Hagen,‡ and Klaus Benndorf*

*Institut für Physiologie II, Friedrich-Schiller-Universität Jena, Jena, Germany; †Fachhochschule Schmalkalden, Fachbereich Elektrotechnik, Schmalkalden, Germany; and ‡Leibniz-Institut für Molekulare Pharmakologie, Berlin, Germany

ABSTRACT Olfactory-type cyclic nucleotide-gated (CNG) ion channels open by the binding of cyclic nucleotides to a binding domain in the C-terminus. Employing the Eyring rate theory, we performed a thermodynamic analysis of the activation gating in homotetrameric CNGA2 channels. Lowering the temperature shifted the concentration-response relationship to lower concentrations, resulting in a decrease of both the enthalpy ΔH and entropy ΔS upon channel opening, suggesting that the order of an open CNGA2 channel plus its environment is higher than that of the closed channel. Activation time courses induced by cGMP concentration jumps were used to study thermodynamics of the transition state. The activation enthalpies $\Delta H^{\ddagger}$ were positive at all cGMP concentrations. In contrast, the activation entropy $\Delta S^{\ddagger}$ was positive at low cGMP concentrations and became then negative at increasing cGMP concentrations. The enthalpic and entropic parts of the activation energies approximately balance each other at all cGMP concentrations, leaving the free enthalpy of activation in the range between 19 and 21 kcal/mol. We conclude that channel activation proceeds through different pathways at different cGMP concentrations. Compared to the unliganded channel, low cGMP concentrations generate a transitional state of lower order whereas high cGMP concentrations generate a transitional state of higher order.

INTRODUCTION

The gating of cyclic nucleotide-gated (CNG) ion channels contributes to the receptor potential of photoreceptors and olfactory neurons (1,2). Native CNG channels are tetrameric proteins composed of either two or three homolog subunits (3–8). One type of subunit of each native channel also forms functional channels on its own when expressed in heterologous systems. Each subunit contains a cyclic nucleotide-binding domain in its C-terminus (9) whose crystal structure has been resolved for related HCN2 channels (10). The channels are activated when these binding domains are occupied by cyclic nucleotides. Because the Hill coefficients for channel activation are between 1.5 and 3.5 (2), it is clear that more than one cyclic nucleotide must bind to a channel to gain maximal opening.

Because CNG channels were shown to open also in the absence of any activating ligand (11,12), cyclic allosteric models were proposed, such as the Monod-Wyman-Changeux (MWC) model (13). The MWC model assumes that a tetrameric CNG channel has four equivalent binding sites and that the ligand affinity in the open states exceeds that in the closed states by an allosteric factor f (for review see (14)). However, when one, two, three, or four cGMP molecules are covalently bound to a CNGA1 channel, the open probabilities for the partially liganded channels were not in the ratios predicted by the MWC model (15). Moreover, experiments in CNGA1 channels suggest that activation proceeds as an action of a dimer of dimers (16).

In contrast to this, the gating of single homotetrameric CNGA2 channels has been described by highly cooperative binding where one or two ligands bind to the closed channel and a further ligand binds to the open channel (17). When studying activation time courses of CNGA2 currents, evoked by cyclic-nucleotide concentration jumps, we showed that an adequate kinetic model requires at least three binding steps and that the binding sites strongly interact (18). In extension of these experiments, we recently measured the activation of CNGA2 channels and the ligand binding simultaneously (19). We showed that indeed four ligands bind to the homotetrameric channel and that the binding sites strongly interact: Binding of the first ligand causes an open probability of ~4%, whereas the binding of the second ligand already opens the channel maximally. Because the association constant of the second binding step is by three orders-of-magnitude smaller than that of the other three binding steps, this step controls the channel activity critically (19).

Additional insight into the physical nature of the activation process of ion channels can be obtained when studying currents at different temperatures because the rates of different conformational changes underlying the activation process can depend on the temperature in a different way. Furthermore, when simplifying the complex activation kinetics to a model consisting of an open and a closed state only and applying the Eyring rate theory (20), it is possible to estimate enthalpic and entropic energy contributions associated with the total activation gating. This has been performed for the transition state, e.g., in voltage-gated K^+ channels (21–24),

Submitted February 19, 2008, and accepted for publication May 29, 2008.

Address reprint requests to Klaus Benndorf, E-mail: klaus.benndorf@mti.uni-jena.de.

Editor: Francisco Bezanilla.

0006-3495/08/09/2750/09 $2.00

doi: 10.1529/biophysj.108.129718

voltage-gated Na^+ channels (25), and K_{ATP} channels (26), and also for energy differences between the closed and the open state itself, e.g., in voltage-gated Na^+ channels (27), CNG channels (28), and cystic fibrosis transmembrane conductance regulator (CFTR) channels (29).

Herein we studied enthalpic and entropic changes associated with the activation of homotetrameric CNGA2 channels for both steady-state conditions and activation time courses after steplike jumps of the cGMP concentration. We show that the entropy of the open channel is smaller than that of the closed channel and, in combination with the results of a kinetic model with four binding steps and strong interaction of the binding sites (19), we conclude that the binding of the first ligand to the closed channel increases the activation entropy whereas the activation entropy decreases by the binding of the following ligands. Our results indicate that enthalpic and entropic parts of the activation energies approximately balance each other at all cGMP concentrations, keeping the free enthalpy of activation in the range between 19 and 21 kcal/mol. Implications for the gating of CNGA2 channels are discussed.

METHODS

Oocyte preparation and cRNA injection

Oocytes were obtained surgically from adult females of *Xenopus laevis* and treated for 60–90 min with 1.2 mg/ml collagenase (Type I, Sigma, St. Louis, MO). The oocytes were manually dissected and injected with 40–70 nl of a solution containing cRNA encoding bovine CNGA2 channels (accession No. X55010). The oocytes were incubated at 18°C in Barth medium until experimental use within six days after injection.

Chemicals

All chemicals were of analytical grade. cGMP was obtained from Sigma. As caged cGMP we used the [7-(diethylamino)coumarin-4-yl]methyl ester of cGMP (DEACMcGMP) (30). A light flash in the wavelength range of 320–480 nm was used to activate DEACMcGMP and liberate cGMP. Photolysis of the DEACMcGMP derivate was fast with respect to the time course of CNGA2 channel activation. In our setup, the kinetics of the photolysis reaction was mainly determined by the time course of the flash lamp pulse and not by the kinetics of the photolysis reaction itself. Photolysis of the caged compounds was completed within 150 μs and was therefore not limiting for the activation time course of CNGA2 channels (18).

Recording of currents

Currents were recorded in inside-out patches with a patch-clamp technique. The patch pipettes were pulled from quartz tubing (outer diameter 1.0 mm, inner diameter 0.7 mm (macroscopic currents) or 0.5 mm (single-channel experiments) using a laser puller (P-2000, Sutter Instrument, Novato, CA). The pipette resistance was 0.8–2.5 MΩ or 5–25 MΩ, respectively. Recording was performed with an Axopatch 200B amplifier (Molecular Devices, Sunnyvale, CA). All experiments were performed with the same recording solution in the bath and the pipette containing (in mM) 150 KCl, 1 EGTA, 5 HEPES. pH was adjusted to 7.4 with KOH. To test for possible background channel activity, each excised patch was first exposed to a solution containing no cyclic nucleotide. Then the maximum current was activated with free cyclic nucleotide (100 μM cGMP). The currents were measured at a voltage of +100 mV.

Concentration jumps of cGMP were exerted by flash photolysis of DEACMcGMP. The experimental setup was the same as that described previously (18). Light flashes, generated by the flash-lamp system JML-C2 (Rapp OptoElectronic, Hamburg, Germany), were directed to the experimental chamber by a quartz light guide. The temperature was kept at 20.3 ± 0.1°C, 15.3 ± 0.1°C, or 10.3 ± 0.1°C by a thermostat. The interval between the flashes was 10–25 s. The concentration of the free cyclic nucleotide produced by flash photolysis was determined by means of the concentration-response relationship obtained at each temperature with free cGMP (18).

Steady-state concentration response relationships were determined with free cGMP under quasi steady-state conditions by applying temperature ramps from 20.0 to 10.0°C within 10 min by means of a Peltier temperature controller (Dagan, Minneapolis, MN). Consequently, all data points were obtained from the same patches. This approach allowed us to identify small temperature effects.

When changing the temperature of a patch, not only the gating of the channel is altered but also the amplitude of the single-channel current and the conductance of the recording system, including the Ag/AgCl electrode in the bath. To isolate the effects of the temperature on the gating during a temperature ramp experiment, we performed the following correction: We determined the open probability (P_o) by single-channel recording at 20.0°C and 10.0°C at a saturating cGMP concentration of 100 μM. The values of P_o were indistinguishable (0.99 ± 0.001 at 20.0°C ($n = 5$) and 0.98 ± 0.008 at 10.0°C ($n = 6$)). We then recorded macroscopic currents from 11 patches with the same saturating cGMP concentration of 100 μM at temperature ramps running from 20.0 to 10.0°C. The current amplitude, $I(100\ \mu M, \vartheta)$, recorded at each degree centigrade, decreased to lower temperatures.

The current amplitude was then normalized with respect to the current amplitude at 20.0°C. The normalized values obtained from all patches were averaged, yielding for each temperature $\vartheta < 20$°C a specific factor $f(\vartheta) = I(100\ \mu M, \vartheta)/I(100\ \mu M, 20°C) < 1$ (Fig. 1 *B*). Because maximum P_o is de facto constant at saturating cGMP concentrations in the considered temperature range (see above), all nonlinear effects of temperature could be attributed to the single-channel current amplitude and the conductance of the recording system. Hence, to isolate at subsaturating cGMP the effects of the temperature on the gating, each measured current, $I(c, \vartheta)$, at a temperature $\vartheta < 20$°C was corrected by multiplication with $1/f$ (Fig. 1, *A* and *C*).

Data acquisition and analysis

Measurements were controlled and data were collected with the ISO3 soft- and hardware (MFK, Niedernhausen, Germany) running on a Pentium PC. For macroscopic currents the sampling rate was generally 2 kHz (filter 1 kHz). Curves were fitted to the data with nonlinear approximation algorithms using either the ISO3 or the Origin 6.1 (OriginLab, Northampton, MA) software. Statistical data are given as mean ± SE.

RESULTS

We first tested the effect of temperature on the concentration-response relationship of the steady-state current, which was measured during slow temperature ramps (see Methods). The steady-state currents, $I(c, \vartheta)$, at different cGMP concentrations, c, were corrected as described in Methods and normalized with respect to the current at 20°C, $I(c, 20°C)$ (Fig. 1 *D*). The plot shows clearly that the temperature effect is very systematic and more pronounced at the lower cGMP concentrations.

In Fig. 2 *A* the corrected currents were normalized with respect to the current at 100 μM cGMP, $I(100\ \mu M, \vartheta)$ in the same patch. The result is that lowering the temperature promotes opening by shifting the concentration-response relationship to lower concentrations.

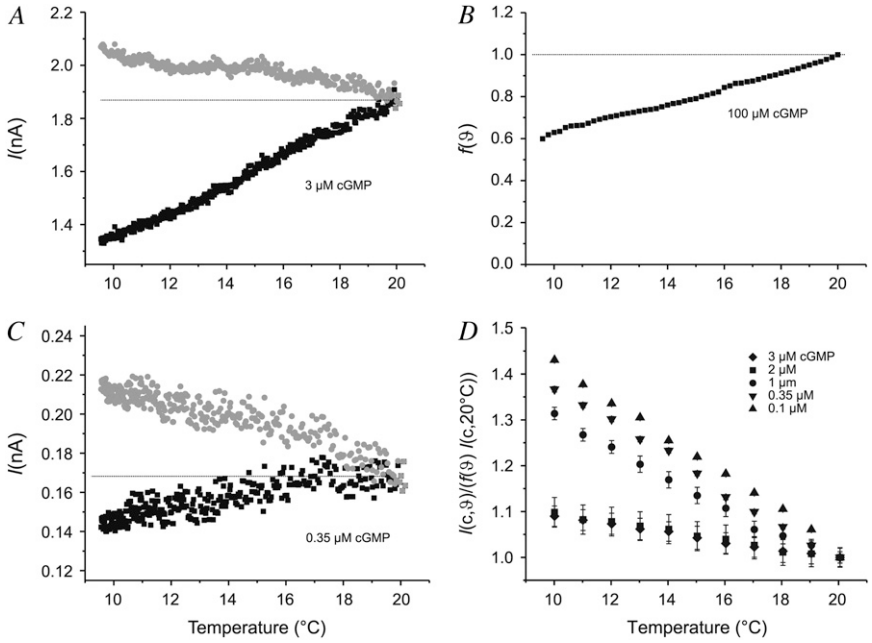

FIGURE 1 Effect of temperature on CNGA2 currents. (*A*) Effect of temperature on CNGA2 currents activated by 3 μM cGMP. Solid symbols indicate the currents that were measured in a representative patch at a cGMP concentration of 3 μM during a temperature ramp from 20.0 to 10.0°C. Current amplitudes that are corrected for the effects of the temperature on the single-channel current amplitude and the recording system (see Methods) are indicated by shaded symbols. (*B*) Effect of temperature on CNGA2 currents at saturating concentration. CNGA2 currents were measured at a cGMP concentration of 100 μM during a temperature ramp from ϑ = 20°C to 10.0°C and normalized with respect to the current amplitude at 20.0°C. Each data point represents the average of 11 patches. The ratio $f(\vartheta) = I(100\ \mu\text{M}, \vartheta)\ /\ I(100\ \mu\text{M}, 20°\text{C})$ is used to correct current amplitudes for the effects of the temperature on the single-channel current and the recordings system (see Methods). (*C*) Effect of temperature on CNGA2 currents in a representative patch activated by 0.35 μM cGMP. Measured and corrected currents are represented by solid and shaded symbols, respectively. (*D*) Corrected and normalized CNGA2 currents as function of temperature. The current amplitudes $I(c, \vartheta)$ were corrected for the effects of the temperature on the single-channel current amplitude and the recordings system and normalized with respect to the current measured at 20.0°C, $I(c,20°C)$ (see Methods). The plot shows that the effect of temperature is more pronounced at lower cGMP concentrations.

For thermodynamic interpretation of these results we considered a simple two-state gating model with n cGMP molecules and infinite cooperativity

$$C + n \times \text{cGMP} \leftrightarrows \text{O(cGMP)}_n, \qquad \text{(Scheme 1)}$$

where C is the unliganded closed and O the liganded open state of the channel. According to the law of mass action, the equilibrium can be characterized by the equilibrium association constant K_A according to $K_A = P_o/\{(1 - P_o)\times\ [\text{cGMP}]^n\}$ where P_o is the open probability. P_o can be approximated by I/I_{max} because at saturating cGMP P_o approximates unity (see Methods). The concentration-response relationships were fitted with the Hill equation

$$I/I_{max} = 1/\{1 + 1/(K_A \times [\text{cGMP}]^n)\}, \qquad (1)$$

yielding K_A and n. Recalling that in the equilibrium

$$\ln K_A = -\Delta H/RT + \Delta S/R, \qquad (2)$$

plotting $\ln K_A$ as function of $1/T$ (van' t Hoff plot; Fig. 2 *B*) allows us to determine the enthalpy ΔH and the entropy ΔS associated with ligand binding and channel opening from the slope and the *y*-intercept, respectively. It should be noted that in this approach both ΔH and ΔS are not exclusively related to the conformational changes of the channel protein but to the entire system comprising the channel, the ligand, and the surrounding water molecules. Furthermore, the temperature dependence of the chemical standard potentials of all molecules involved was assumed to be negligible.

The result is that, under steady-state conditions, channel opening is associated with a decrease of both enthalpy ($\Delta H = -11.2$ kcal M^{-1}) and entropy ($\Delta S = -38.1$ cal M^{-1} K^{-1}). The resulting free enthalpy $\Delta G = \Delta H - T\Delta S$ is negligible (-0.03 kcal M^{-1} at 20°C). This result is a prerequisite for a reversible system: All enthalpy change inferred by the cGMP binding decreases the entropy of the channel (including that of the ligands and the environment) and vice versa.

The results so far considered equilibrium thermodynamic changes of CNGA2 channel opening associated with the transfer of energy from the ligand to the channel but did not consider those thermodynamic changes associated with the time-dependent activation process elicited by stepping cGMP from zero to a constant cGMP level. We therefore studied the activation time course of CNGA2 currents by cGMP concentration jumps produced by flash photolysis of a caged cGMP (see Methods). Fig. 3 *A* shows representative current recordings at 20.3°C. As reported previously (18), these time courses can be fully described with the sum of two exponentials,

$$I = A_{fast}\exp(-t/\tau_{fast}) + A_{slow}\exp(-t/\tau_{slow}), \qquad (3)$$

yielding the respective current components and time constants. These time constants do not depend on the cGMP concentration in a monotonic but in a complicated fashion: They are slow at the lowest measurable cGMP concentration, and near the EC_{50} value, are faster in-between, and considerably accelerated at high cGMP concentrations (*circles* in Fig. 4 *A*). Because the concentration-response relationships are slightly different at different temperatures (see above), we normalized the cGMP concentration in all diagrams upon cGMP concentration jumps to the EC_{50} value, which is the

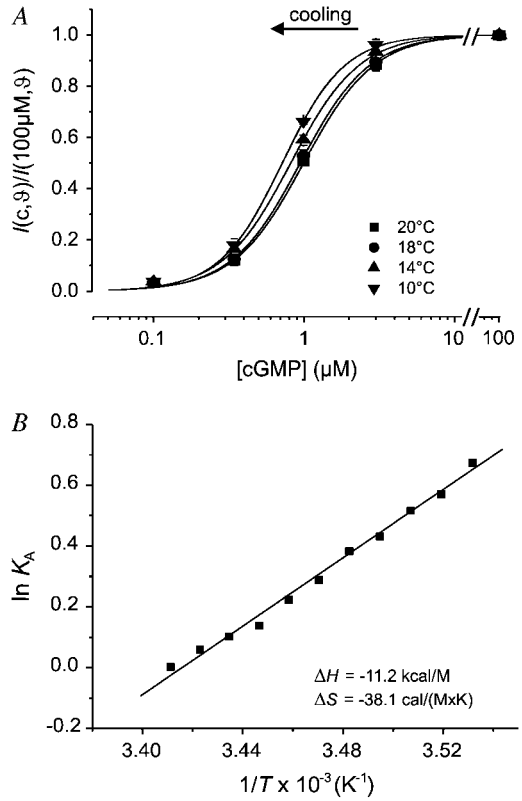

FIGURE 2 Thermodynamic analysis of CNGA2 channels under steady-state conditions. (*A*) Concentration-response relationship of CNGA2 currents at four temperatures. The current amplitudes $I(c, \vartheta)$ were normalized with respect to the current amplitude at the saturating concentration of 100 μM cGMP, $I(100\ \mu M, \vartheta)$. The data points were fitted with the Hill equation (Eq. 1), yielding as parameters at 20.0°C: $K_A = 0.994\ \mu M^{-n}$, $n = 1.86$; at 18.0°C: $K_A = 0.902\ \mu M^{-n}$, $n = 1.88$; at 14.0°C: $K_A = 0.681\ \mu M^{-n}$, $n = 1.91$; and at 10.0°C: $K_A = 0.503\ \mu M^{-n}$, $n = 2.09$. Cooling shifts the relationships to lower cGMP concentrations. (*B*) van' t Hoff plot. $\ln K_A$ was plotted as a function of $1/T$, yielding $\Delta H = -11.2$ kcal M^{-1} and $\Delta S = -38.1$ cal M^{-1} K^{-1}.

cGMP concentration generating half-maximum current. It is related to K_A by $EC_{50} = K_A^{-1/n}$ (31).

At the lower temperature of 10.3°C, the activation time courses are slower compared to those obtained at similar cGMP concentrations at 20.3°C (Fig. 3 *B*). When plotting the time constants as function of the cGMP concentration, it becomes obvious that the low temperature decelerates activation more at low than at high cGMP (*squares* in Fig. 4 *A*). To demonstrate this more explicitly, we calculated the temperature coefficient $Q_{10} = \tau_{103°C}/\tau_{203°C}$ for both τ_{fast} and τ_{slow} and plotted these values as function of [cGMP]/EC_{50} (Fig. 4 *B*). The Q_{10} value is maximal near [cGMP]/EC_{50} = 0.1 and decays steeply to higher cGMP concentrations with an additional small local maximum near [cGMP]/$EC_{50} = 1$. Since $\ln(Q_{10})$ is proportional to the activation energy (32), these results suggest that at [cGMP]/EC_{50} near 0.1, channel opening requires us to overcome a significantly higher energy barrier than at higher concentrations.

For further thermodynamic interpretation of the activation time course, we assumed that at each cGMP concentration only one closed-open transition dominates the activation kinetics and that the ligand binding is not rate-limiting (18,19). For the sake of simplicity, we quantified the overall speed of the activation time course by the mean activation time constant τ_{mean}:

$$\tau_{mean} = (A_{fast}\tau_{fast} + A_{slow}\tau_{slow})/(A_{fast} + A_{slow}). \quad (4)$$

The plot of τ_{mean} as a function of [cGMP]/EC_{50} (Fig. 4 *C*) shows a similar profile to that of the individual time constants (see Fig. 4 *A*). Also the Q_{10} value derived from τ_{mean} was maximal at [cGMP]/EC_{50} near 0.1 and decreased to the higher cGMP concentrations. Hence, τ_{mean} can be considered a reasonable parameter for describing the overall activation speed.

Because it is possible to interpret an inverse time constant as a rate constant (22,24,33), we used $k = 1/\tau_{mean}$ as the rate constant characterizing the overall activation. The temperature dependency of this rate constant k was studied by the Arrhenius equation

$$\ln k = \ln A_a - E_a/(RT), \quad (5)$$

where A_a is a preexponential factor, E_a the activation energy, R the molar gas constant, and T the absolute temperature. Arrhenius plots ($\ln k$ versus $1/T$) were built over a wide range of cGMP concentrations (Fig. 5). In these plots, we also included data obtained at 15.3°C to prove that the relationships are linear in the considered temperature range of 10.3 and 20.3°C. From the slope in the Arrhenius plots, we determined E_a. As expected from the Q_{10} values, this plot also showed a pronounced maximum near [cGMP]/EC_{50} = 0.1 and a local maximum near [cGMP]/$EC_{50} = 1$ (Fig. 6 *A*).

According to the transition-state theory, the rate constant of the activation step is related to the Gibbs free activation enthalpy ($\Delta G^{\ddagger}$) by

$$k = \kappa\frac{k_B T}{h}\exp(-\Delta G^{\ddagger}/RT), \quad (6)$$

where k_B is the Boltzmann constant, h the Planck constant, and κ the transmission coefficient set to unity (34). $\Delta G^{\ddagger}$ can be obtained by rearranging Eq. 6 as

$$\Delta G^{\ddagger} = -RT\ln\left(\frac{kh}{k_B T}\right). \quad (7)$$

The resulting dependency of $\Delta G^{\ddagger}$ on [cGMP]/EC_{50} (calculated for 20.3°C) is of similar shape as the time constant for activation (Fig. 6 *B*).

The free activation enthalpy $\Delta G^{\ddagger}$ consists of an enthalpic ($\Delta H^{\ddagger}$) and an entropic component, ($T\Delta S^{\ddagger}$),

$$\Delta G^{\ddagger} = \Delta H^{\ddagger} - T\Delta S^{\ddagger}. \quad (8)$$

The activation enthalpy $\Delta H^{\ddagger}$ was obtained from the activation energy E_a by

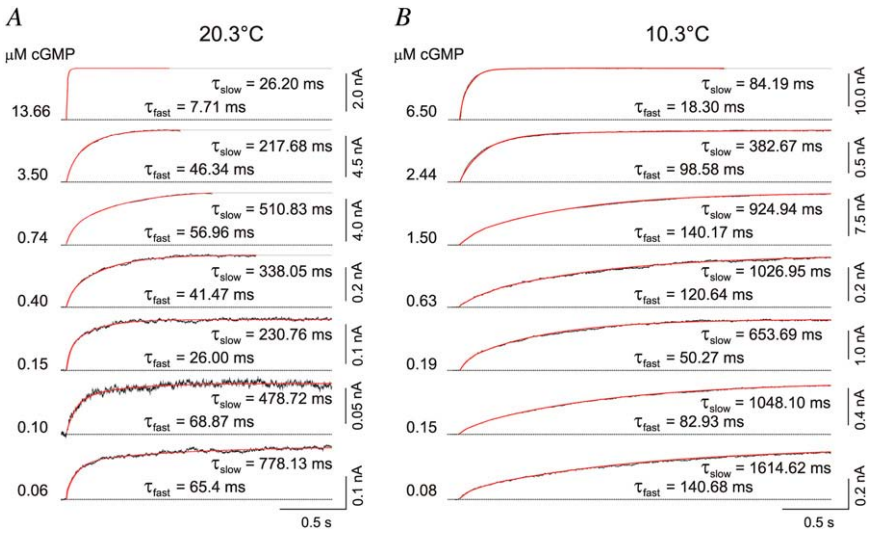

FIGURE 3 Activation time courses of CNGA2 currents elicited by cGMP jumps. (*A*) Activation time courses at 20.3°C. (*B*) Activation time courses at 10.3°C. Activation time courses were obtained from different patches at the indicated cGMP concentrations. The traces were fitted (*red curves*) with the sum of two exponentials (Eq. 3) yielding the indicated time constants τ_{fast} and τ_{slow}. For comparison, the traces were selected such that the cGMP concentrations of two traces side by side are similar.

$$\Delta H^{\ddagger} = E_a - RT, \tag{9}$$

and the activation entropy $\Delta S^{\ddagger}$ by

$$\Delta S^{\ddagger} = (\Delta H^{\ddagger} - \Delta G^{\ddagger})/T. \tag{10}$$

$\Delta H^{\ddagger}$ was positive at all cGMP concentrations and depends, of course, in the same way on [cGMP]/EC_{50} as E_a (Fig. 6 *C*). The $\Delta H^{\ddagger}$ difference between the smallest and largest measured cGMP concentration, $\Delta\Delta H^{\ddagger}$, was −13.4 kcal M^{-1}.

Particularly noteworthy is the dependency of $\Delta S^{\ddagger}$ on [cGMP]/EC_{50} (Fig. 6 *D*): At low [cGMP], $\Delta S^{\ddagger}$ is positive, suggesting that at these concentrations, where only one of the four binding sites is occupied (see Discussion), the transition state of the protein is characterized by increased disorder, presumably due to reduced intramolecular interactions. Toward higher concentrations, $\Delta S^{\ddagger}$ decreases. Hence, an increasing degree of binding of the ligand promotes an increase of order in the transition state which can be interpreted as enhanced intramolecular interactions. The $\Delta S^{\ddagger}$ difference between the smallest and largest cGMP concentration, $\Delta\Delta S^{\ddagger}$, is in the range of ΔS determined from steady-state data (−42.8 kcal M^{-1} K^{-1} vs. −38.1 kcal M^{-1} K^{-1}).

The free activation enthalpy $\Delta G^{\ddagger}$ is in the range of 20 kcal M^{-1} and depends on the cGMP concentration only mildly (Fig. 6 *B*) in contrast to $\Delta H^{\ddagger}$ and $\Delta S^{\ddagger}$ (Fig. 6, *C* and *D*). Similar to the enthalpy and entropy differences between the open and closed state under steady-state conditions, the differences for the transition state between high and low cGMP

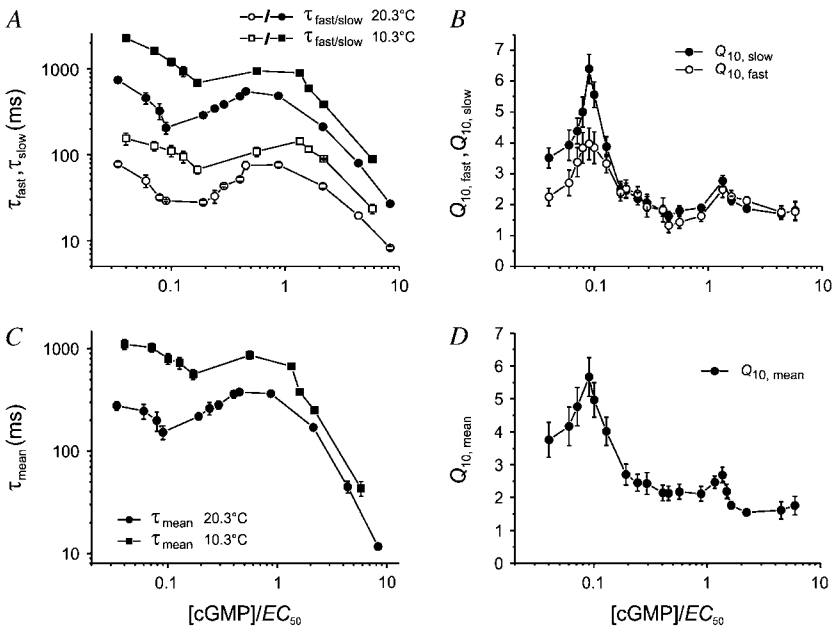

FIGURE 4 Temperature dependence of the speed of activation on the cGMP concentration. (*A*) Plot of the activation time constants τ_{fast} and τ_{slow} as function of the cGMP concentration at 20.3 and 10.3°C. Each data point was obtained from 5 to 20 patches. Here and in the following diagrams, the cGMP concentration was normalized to the EC_{50} value, which was 1.64 μM at 20.3°C and 1.12 μM at 10.3°C, respectively. The speed of activation was fast at high cGMP and slow at low cGMP but did not depend on the cGMP concentration in a simple monotonous fashion. (*B*) Plot of the temperature coefficients $Q_{10,fast} = \tau_{fast}^{10.3°C}/\tau_{fast}^{20.3°C}$ and $Q_{10,slow} = \tau_{slow}^{10.3°C}/\tau_{slow}^{20.3°C}$ as function of [cGMP]/EC_{50}. At cGMP concentrations where time constants were only available for one temperature, the time constants for the other temperature were obtained by linear interpolation. Both time constants generate a maximum Q_{10} at [cGMP]/EC_{50} near 0.1. (*C*) Mean activation time constant τ_{mean} as function of [cGMP]/EC_{50} at 20.3 and 10.3°C. The value τ_{mean} was calculated according to Eq. 4. The profile is similar to that of the individual time constants. (*D*) Temperature coefficient Q_{10} for τ_{mean} as function of [cGMP]/EC_{50}. Similar to Q_{10} for the individual time constants, also $Q_{10,mean}$ exhibits a maximum at [cGMP]/EC_{50} near 0.1.

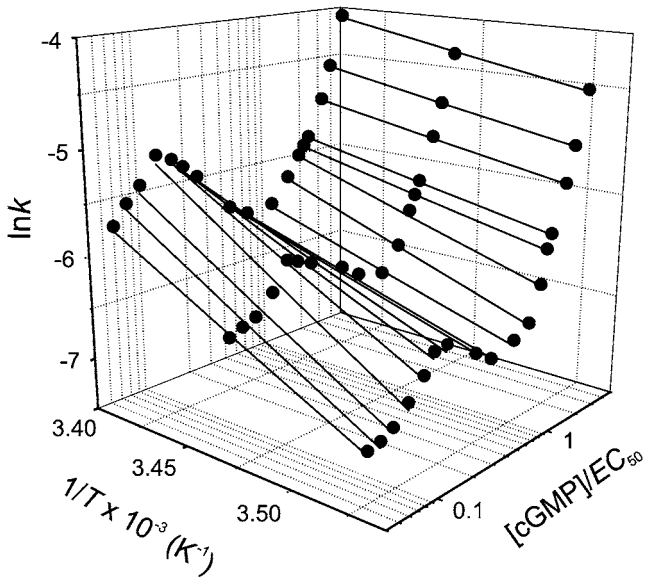

FIGURE 5 Arrhenius plots of the activation rate constants of CNGA2 currents over a wide range of cGMP concentrations. The activation rate, k, was obtained from the reciprocal mean activation time constant, τ_{mean}, at the temperatures 20.3, 15.3, and 10.3°C. At each cGMP concentration ln$k$ is plotted as function of the reciprocal temperature $1/T$ and the three data points were fitted by a straight line, yielding the activation energy E_a. Error bars (see Fig. 4 *C*) were omitted for clarity.

concentrations are negative ($\Delta\Delta H^{\ddagger} = -13.4$ kcal M^{-1}, $\Delta\Delta S^{\ddagger} = -42.8$ cal M^{-1} K^{-1}). However, the free activation enthalpy difference $\Delta\Delta G^{\ddagger} = \Delta\Delta H^{\ddagger} - T\Delta\Delta S^{\ddagger} = -0.8$ kcal M^{-1} (calculated for 20.3°C) is close to zero. This indicates that the barrier of free activation enthalpy, which has to be overcome, is almost the same at all cGMP concentrations. Only the enthalpic and entropic contributions to the free activation enthalpy differ considerably at low and high cGMP concentrations.

DISCUSSION

The thermodynamic analysis of CNGA2 channels in this study shows that these channels undergo highly temperature-dependent conformational changes. From the dose-response relationships at different temperatures, we were able to calculate the differences of the Gibbs free enthalpy ΔG, the enthalpy ΔH, and the entropy ΔS between the endpoints of the channel activation pathway, i.e., between the unliganded closed and the liganded open state. It should be noted that these extensive thermodynamic variables apply to the entire system comprising the channel, the ligand, and solvating water molecules. The overall free enthalpy of cGMP binding can be theoretically split into three components: 1), the amount of free enthalpy that is necessary to separate the dissolved ligand from the surrounding water molecules; 2), the amount of free enthalpy that is associated with the binding of the free, unhydrated ligand to the cyclic nucleotide binding site; and 3), the amount of free enthalpy associated with subsequent conformational changes of the channel protein. The same applies for the other extensive variables such as the enthalpy and the entropy. Based on our previous results that the ligand binding is much faster than the conformational changes associated with channel opening (18,19), the enthalpies and entropies determined herein can be essentially attributed to the conformational changes only.

The van' t Hoff plot (Fig. 2 *B*) yielded the result that, under steady-state conditions, channel opening is associated with a decrease of both enthalpy ($\Delta H = 11.2$ kcal M^{-1}) and entropy ($\Delta S = -38.1$ cal M^{-1} K^{-1}). The resulting free enthalpy $\Delta G = \Delta H - T\Delta S$ is negligible (-0.03 kcal M^{-1}). Thus, the entropy of the open channel is smaller than the entropy of the closed channel. This result is in line with results of other reports, e.g., in voltage-gated Na^+ channels (25,27), cystic fibrosis transmembrane conductance regulator (CFTR (29)),

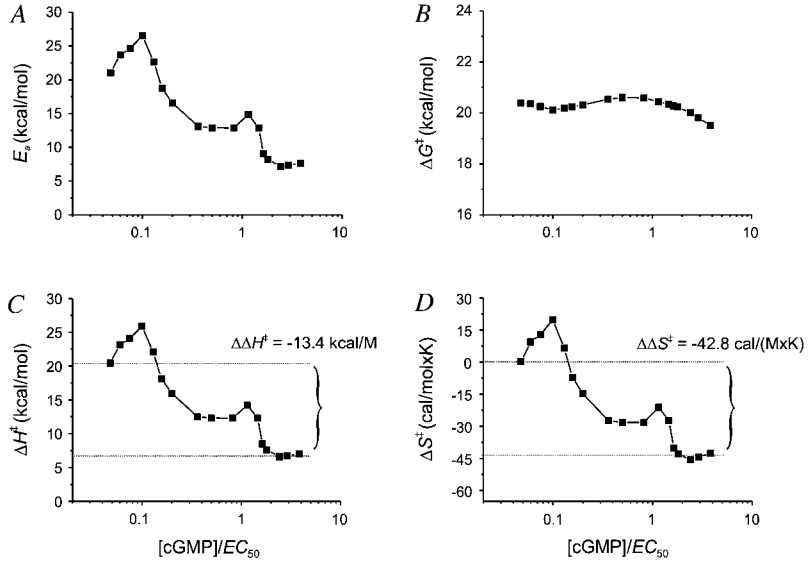

FIGURE 6 Thermodynamics of cGMP-jump induced activation of CNGA2 channels as function of the cGMP concentration. (*A*) Plot of the activation energy E_a, as function of [cGMP]/EC_{50}. E_a was obtained from the slope in the Arrhenius plots (Fig. 5). (*B*) Plot of the free activation enthalpy $\Delta G^{\ddagger}$ as function of [cGMP]/EC_{50}. $\Delta G^{\ddagger}$ was calculated by Eq. 7. (*C*) Plot of the activation enthalpy $\Delta H^{\ddagger}$ as function of [cGMP]/EC_{50}. $\Delta H^{\ddagger}$ was calculated by Eq. 9. $\Delta\Delta H^{\ddagger}$ is the difference between $\Delta H^{\ddagger}$ at the highest and lowest cGMP concentration. (*D*) Plot of the activation entropy $\Delta S^{\ddagger}$ as function of [cGMP]/EC_{50}. $\Delta S^{\ddagger}$ was calculated by Eq. 10. The entropy is only positive at very low cGMP. $\Delta\Delta S^{\ddagger}$ is the difference between $\Delta S^{\ddagger}$ at the highest and lowest cGMP concentration.

and cold receptor TRPM8 (33). In contrast, positive entropy changes with channel opening were determined for native voltage-gated K^+ channels (21,23). Moreover, both positive and negative entropies were reported for the opening of ATP sensitive K^+ channels (K_{ATP} channels) in different temperature ranges (26) and for different components of hyperpolarization-activated currents (I_h) in primary sensory neurons (35). Knowing that voltage-dependent channels and CNG channels are structurally related, and that the pore of K_{ATP} channels has structural similarities with that of CNG and voltage-dependent channels, it is somewhat surprising that entropy changes associated with channel opening are either positive or negative. Particularly challenging are the opposite entropy changes observed herein for CNGA2 channels and those for HCN channels, generating I_h (35), because these channel types are close relatives (36). To learn more about the differences in the gating it would therefore be desirable to determine these entropy changes in defined recombinant HCN channels under otherwise identical experimental conditions.

The activation time courses produced by cGMP concentration jumps from zero to different concentrations yielded additional valuable information upon the activation of the channels. Here, the extensive thermodynamic variables of the transition states are compared with those of the unliganded closed state. How can these results be related to our previous results where we proposed a much more detailed kinetic model to describe the gating of CNGA2 channels (19)? Fig. 7 *A* illustrates our favored C4L model with all equilibrium constants indicated. According to this model a channel can bind four ligands, but the binding of the second ligand is the most critical step for activation because it switches the channel from mainly closed to mainly open. Fig. 7 *B* shows the degree of liganding of the channel protein as a function of the cGMP concentration according to the C4L model. At low cGMP concentrations, the probability of being in the unliganded closed (C_0) or unliganded open (O_0) state is close to unity. Increasing the cGMP concentration leads to progressive liganding with higher numbers of bound ligands, resulting finally in the population of the fully liganded closed (C_4) or open (O_4) state.

Most notable with respect to the results of this study is that, at cGMP/$EC_{50} < 0.1$, only the single-liganded states C_1+O_1, together with the nonliganded states, C_0+O_0, but not the higher liganded states, are populated. Hence, at cGMP/$EC_{50} < 0.1$, the activation time courses by cGMP jumps are most likely dominated by the closed-open transition $C_1 \leftrightarrows O_1$ of the single-liganded channel (19). The activation enthalpy $\Delta H^{\ddagger}$ of this transition is positive, but partially balanced by an increase in entropy (Fig. 6, *C* and *D*), resulting in a free activation enthalpy $\Delta G^{\ddagger}$ near 20 kcal/mol. For further increasing cGMP/EC_{50}, the closed-open transitions of the double-, triple-, and fully liganded channel contribute progressively more to the activation. $\Delta H^{\ddagger}$ is lower at these concentrations (Fig. 6 *C*). This indicates that another pathway

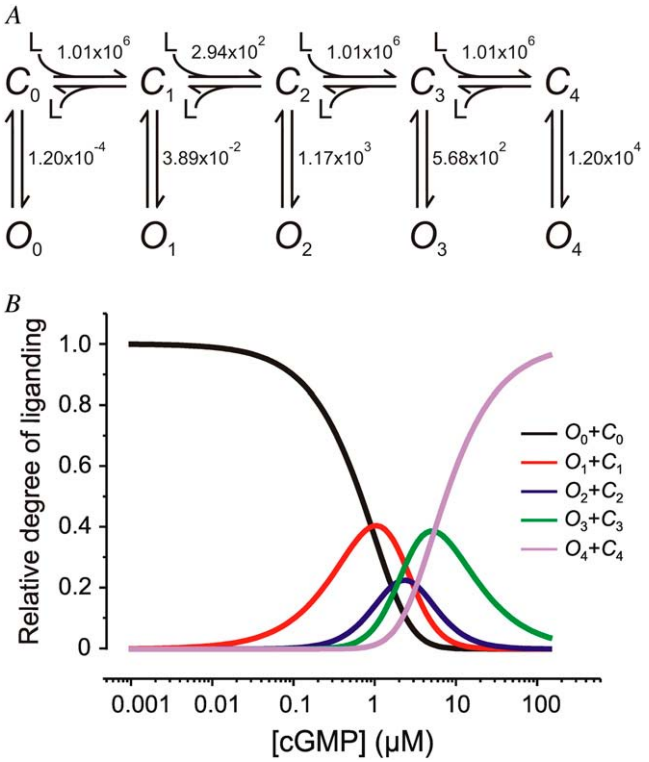

FIGURE 7 Degree of liganding as function of the cGMP concentration according to the C4L model proposed by Biskup et al. (19). (*A*) Scheme of the C4L model. The model consists of five closed states ($C_0 \ldots C_4$) and five open states ($O_0 \ldots O_4$). The equilibrium association constants are indicated in M^{-1} (*horizontal reactions*); the closed-open isomerization constants are dimensionless (*vertical reactions*). (*B*) Plot of the degree of liganding with respect to the sum of all degrees of liganding as a function of [cGMP]/EC_{50}. The degrees of liganding add to unity at each cGMP concentration. At [cGMP]/$EC_{50} < 0.1$, only the single-liganded state (C_1+O_1) contributes to channel opening.

is involved in channel opening. If at higher concentrations the channel would open significantly via $C_1 \leftrightarrows O_1$, $\Delta H^{\ddagger}$ should be the same as at cGMP/$EC_{50} < 0.1$, which is not the case. This confirms the absence of a major transition between O_2 and O_3, as proposed in our previous studies (18,19). Thus, at higher cGMP concentrations, the channel opens from either C_2, C_3, or C_4.

Interestingly, the activation entropy $\Delta S^{\ddagger}$ has a similar profile along the cGMP/EC_{50} axis as $\Delta H^{\ddagger}$. Its values are positive at cGMP/$EC_{50} < 0.1$ and then decrease to higher cGMP concentrations. Together with the computed curves in Fig. 7 *B*, this result suggests that the binding of only one ligand possibly increases the protein flexibility, and thus the entropy. At higher cGMP concentrations, when more than one ligand is bound, the channel is driven to a more ordered transition state. The negative entropy associated with the binding of the second, third, and fourth ligand is produced at the expense of $\Delta H^{\ddagger}$.

At low cGMP concentrations, $\Delta S^{\ddagger}$ is close to zero, indicating that the entropy of the transition state is close to the

entropy of the unliganded closed state. This suggests that along the reaction pathway the transition state is also structurally similar to the unliganded closed state. At high cGMP concentrations, $\Delta S^{\ddagger}$ is close to the entropy of the open channel. This indicates that the entropy of the transition state is close to the entropy of the state of the open channel. This suggests that, along the reaction pathway, the transition state is also structurally similar to the state of the open channel.

A local maximum in the decreasing profile of $\Delta H^{\ddagger}$ and $\Delta S^{\ddagger}$ to higher cGMP concentrations exists near the EC_{50} value (Fig. 6 *C*). If the absolute maximum in $\Delta S^{\ddagger}$ at low cGMP is caused by an entropy increase produced by the binding of the first ligand, it is possible that near the EC_{50} value, another increase of entropy appears, overlapping the general entropy decrease with increasing cGMP concentrations. This local increase in entropy might be generated by a loss of intramolecular interaction during the extensive conformational changes associated with activation.

Despite this obvious match of the energetic considerations studied herein and the curves of Fig. 7 *B* computed with the model derived previously (19), one should be aware that the curves reflect steady-state responses whereas the activation time courses are dynamic responses of the channel for which the energies and entropies were obtained by several strongly simplifying assumptions. It should also be noted that, by methodical reasons, the rate constants in the C4L model were determined for the voltage of +10 mV instead of +100 mV used herein. However, this comparison is viewed to be justified because the effect of voltage on the gating of CNG channels is only very weak. To gain deeper insight into the complex gating mechanism of CNG channels, a good idea would be to further investigate the effects of temperature on the channel function.

We are indebted to U.B. Kaupp, Jülich, for providing the cDNA encoding CNGA2 channels. We thank K. Schoknecht, S. Bernhardt, A. Kolchmeier, and B. Tietsch for excellent technical assistance.

REFERENCES

1. Zagotta, W. N., and S. A. Siegelbaum. 1996. Structure and function of cyclic nucleotide-gated channels. *Annu. Rev. Neurosci.* 19:235–263.
2. Kaupp, U. B., and R. Seifert. 2002. Cyclic nucleotide-gated ion channels. *Physiol. Rev.* 82:769–824.
3. Chen, T. Y., Y. W. Peng, R. S. Dhallan, B. Ahamed, R. R. Reed, and K. W. Yau. 1993. A new subunit of the cyclic nucleotide-gated cation channel in retinal rods. *Nature.* 362:764–767.
4. Körschen, H. G., M. Illing, R. Seifert, F. Sesti, A. Williams, S. Gotzes, C. Colville, F. Müller, A. Dosé, M. Godde, L. L. Molday, U. B. Kaupp, and R. S. Molday. 1995. A 240 kDa protein represents the complete β subunit of the cyclic nucleotide-gated channel from rod photoreceptor. *Neuron.* 15:627–636.
5. Bönigk, W., J. Bradley, F. Muller, F. Sesti, I. Boekhoff, G. V. Ronnett, U. B. Kaupp, and S. Frings. 1999. The native rat olfactory cyclic nucleotide-gated channel is composed of three distinct subunits. *J. Neurosci.* 19:5332–5347.
6. Zheng, J., M. C. Trudeau, and W. N. Zagotta. 2002. Gating rearrangements in cyclic nucleotide-gated channels revealed by patch-clamp fluorometry. *Neuron.* 28:369–374.
7. Weitz, D., N. Ficek, E. Kremmer, P. J. Bauer, and U. B. Kaupp. 2002. Subunit stoichiometry of the CNG channel of rod photoreceptors. *Neuron.* 36:881–889.
8. Zhong, H., L. L. Molday, R. S. Molday, and K. W. Yau. 2002. The heteromeric cyclic nucleotide-gated channel adopts a 3A:1B stoichiometry. *Nature.* 420:193–198.
9. Matulef, K., G. E. Flynn, and W. N. Zagotta. 1999. Molecular rearrangements in the ligand-binding domain of cyclic nucleotide-gated channels. *Neuron.* 24:443–452.
10. Zagotta, W. N., N. B. Olivier, K. D. Black, E. C. Young, R. Olson, and E. Gouaux. 2003. Structural basis for modulation and agonist specificity of HCN pacemaker channels. *Nature.* 425:200–205.
11. Picones, A., and J. I. Korenbrot. 1995. Spontaneous ligand-independent activity of the cGMP-gated ion channels in cone photoreceptors in fish. *J. Physiol.* 485:699–714.
12. Tibbs, G. R., E. H. Goulding, and S. A. Siegelbaum. 1997. Allosteric activation and tuning of ligand efficacy in cyclic-nucleotide-gated channels. *Nature.* 386:612–661.
13. Monod, J., J. Wyman, and J. P. Changeux. 1965. On the nature of allosteric transitions: a plausible model. *J. Mol. Biol.* 12:88–118.
14. Li, J., W. N. Zagotta, and H. A. Lester. 1997. Cyclic-nucleotide gated channels: structural basis of ligand efficacy and allosteric modulation. *Q. Rev. Biophys.* 30:177–193.
15. Ruiz, M. L., and J. W. Karpen. 1997. Single cyclic nucleotide-gated channels locked in different ligand-bound states. *Nature.* 389:389–392.
16. Liu, D. T., G. R. Tibbs, P. Paoletti, and S. A. Siegelbaum. 1998. Constraining ligand binding site stoichiometry suggests that a cyclic nucleotide-gated channel is composed of two functional dimers. *Neuron.* 21:235–248.
17. Li, J., and H. A. Lester. 1999. Single-channel kinetics of the rat olfactory cyclic nucleotide-gated channel expressed in *Xenopus* oocytes. *Mol. Pharmacol.* 55:883–893.
18. Nache, V., E. Schulz, T. Zimmer, J. Kusch, C. Biskup, R. Koopmann, V. Hagen, and K. Benndorf. 2005. Activation of olfactory-type cyclic nucleotide-gated channels is highly cooperative. *J. Physiol.* 569:92–102.
19. Biskup, C., J. Kusch, E. Schulz, V. Nache, F. Schwede, F. Lehmann, V. Hagen, and K. Benndorf. 2007. Relating ligand binding to activation gating in CNGA2 channels. *Nature.* 446:440–443.
20. Glasstone, S., K. J. Laidler, and H. Eyring. 1941. The Theory of Rate Processes. McGraw Hill, New York.
21. Tsien, R. W., and D. Noble. 1969. A transition state theory approach to the kinetics of conductance changes in excitable membranes. *J. Membr. Biol.* 1:248–273.
22. Meyer, R., and S. H. Heinemann. 1997. Temperature and pressure dependence of *Shaker* K^+ channel N-type and C-type inactivation. *Eur. Biophys. J.* 26:433–445.
23. Tiwari, J. K., and S. K. Sikdar. 1999. Temperature-dependent conformational changes in a voltage-gated potassium channel. *Eur. Biophys. J.* 28:338–345.
24. Rodriguez, B. M., D. Sigg, and F. Bezanilla. 1998. Voltage gating of *Shaker* K^+ channels. The effect of temperature on ionic and gating currents. *J. Gen. Physiol.* 112:223–242.
25. Benndorf, K., and R. Koopmann. 1993. Thermodynamic entropy of two conformational transitions of single Na^+ channel molecules. *Biophys. J.* 65:1585–1589.
26. McLarnon, J. G., B. N. Hamman, and G. F. Tibbits. 1993. Temperature dependence of unitary properties of an ATP-dependent potassium channel in cardiac myocytes. *Biophys. J.* 65:2013–2020.
27. Correa, A. M., F. Bezanilla, and R. Latorre. 1992. Gating kinetics of batrachotoxin-modified Na^+ channels in the squid giant axon. Voltage and temperature effects. *Biophys. J.* 61:1332–1352.
28. Bucossi, G., M. Nizzari, and V. Torre. 1997. Single-channel properties of ionic channels gated by cyclic nucleotides. *Biophys. J.* 72:1165–1181.
29. Aleksandrov, A. A., and J. R. Riordan. 1998. Regulation of CFTR ion channel gating by MgATP. *FEBS Lett.* 431:97–101.

30. Hagen, V., J. Bendig, S. Frings, T. Eckardt, S. Helm, D. Reuter, and U. B. Kaupp. 2001. Highly efficient and ultrafast phototriggers for cAMP and cGMP by using long-wavelength UV/Vis-activation. *Angew. Chem. Int. Ed.* 40:1046–1048.

31. Barlow, R., and J. F. Blake. 1989. Hill coefficients and the logistic equation. *Trends Pharmacol. Sci.* 10:440–441.

32. Cota, G., L. Siri, and E. Stefani. 1983. Calcium channel gating in frog skeletal muscle membrane: effect of temperature. *J. Physiol.* 338:395–412.

33. Brauchi, S., P. Orio, and R. Latorre. 2004. Clues to understanding cold sensation: thermodynamics and electrophysiological analysis of the cold receptor TRPM8. *Proc. Natl. Acad. Sci. USA.* 101:15494–15499.

34. Hille, B. 1992. Ionic Channels of Excitable Membranes, 2nd Ed. Sinauer Associates, Sunderland, MA.

35. Pena, F., B. Amuzescu, E. Neaga, and M. L. Flonta. 2006. Thermodynamic properties of hyperpolarization-activated current (I_h) in a subgroup of primary sensory neurons. *Exp. Brain Res.* 173:282–290.

36. Craven, K. B., and W. N. Zagotta. 2006. CNG and HCN channels: Two peas, one pod. *Annu. Rev. Physiol.* 68:375–401.